Imperial College London

Pacific subsurface temperature as a long-range indicator of El Niño, regional precipitation, and fire

Enoch Yan Lok Tsui*[1,2] | Ralf Toumi[1,3]

[1]Department of Physics, Imperial College London, London, UK

[2]Leverhulme Centre for Wildfires, Environment and Society, London, UK

[3]Granthrm Institute, Imperial College London, London, UK

*e.tsui20@imperial.ac.uk

Introduction

El Niño (La Niña) events refer to the warming (cooling) of the equatorial Pacific Ocean sea surface temperature (SST) [1,2]. These conditions are accompanied by a weakening (strengthening) of the Pacific equatorial trade winds and other changes in atmospheric and oceanic circulations [2]. The Southern Oscillation refers to the oscillatory behaviour of the sea-level pressure between the tropical East and West Pacific [1]. The warming and cooling of the equatorial Pacific SST and the Southern Oscillation are now understood as different manifestations of the same basin-wide climate phenomenon termed El Niño-Southern Oscillation (ENSO), which is driven by coupled atmosphere-ocean processes [1,2]. ENSO affects global climate, marine and terrestrial ecosystems [2]. It dominates interannual climate variability and affects seasonal precipitation, wind and temperature patterns over vast distances globally through dynamical atmospheric processes [3,2].

The incorporation of subsurface temperature into statistical ENSO oceanic surface state predictions has been explored previously [e.g. 4–6]. Here we extend the idea to study for the first time directly the relationship between subsurface temperature and the atmospheric responses throughout the tropics identified to have teleconnection with the ENSO oceanic surface state. We do this by proposing the SubNiño4 index similar to the commonly used long-range ENSO predictor of western Pacific warm water volume (WWV_W) [e.g. 7–9].

We showed that the lagged correlation between observed SubNiño4 and Niño 3.4 can exceed the simultaneous correlation between observed and predicted ENSO at a lead time of around 12 months. We also show that the SubNiño4 index may be more reliable than the WWV_W indicator. Using regional precipitations and fires as examples, we demonstrate that the SubNiño4 index can serve as a long-range indicator of ENSO-driven atmospheric phenomena in many regions of the tropics.

The SubNiño4 index

The SubNiño4 index is defined to be the subsurface potential temperature (SubT) anomaly averaged beneath the Niño 4 region (160°E–150°W, 5°S–5°N) and between the depths of 100 and 300 m, around the thermocline. In general, the SubNiño4 index leads that of the Niño 3.4 index by a fairly constant time of about 6 to 12 months (Fig. 1(a)). The frequency spectra of both the Niño 3.4 and SubNiño4 time series have significant peaks corresponding to periods of 1.46 yr and 4.53 yr (Fig. 1(b)). The two frequency spectra are similar overall but SubNiño4 is less noisy, possibly due to a lack of direct atmospheric coupling of the subsurface compared to the surface, making the SubT less prone to influences from high frequency or stochastic atmospheric forcings than the SST. The normalised histograms of the two indices are shown in Fig. 1(c). The SubNiño4 index displays a higher mean, lower standard deviation and higher kurtosis than the Niño 3.4 index. The SubNiño4 index is negatively skewed while the Niño 3.4 index is positively skewed, with the former having a higher absolute skewness.

Indicator of ENSO

The lagged correlations (r) of the SubNiño4 index and the WWV_W anomaly with the Niño 3.4 index over each of the four main seasons (Fig. 2) show that the SubNiño4 index can function as a long-range indicator for ENSO more reliably than the WWV_W anomaly. For a broad time window one year ahead

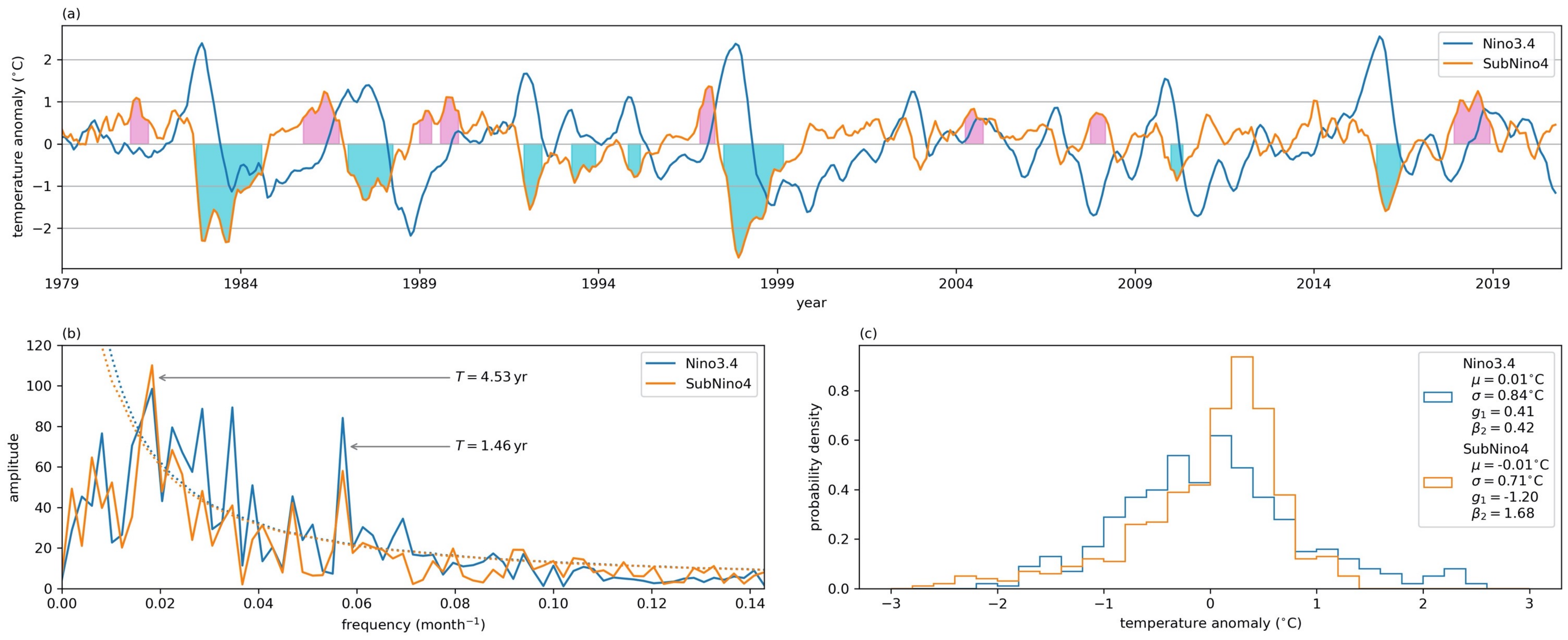

Figure 1 (a) Time series of the SubNiño4 and Niño 3.4 indices. Subsurface warm (cold) events are indicated with pink (cyan) shading. (b) Frequency spectra of SubNiño4 and Niño 3.4. The dashed lines indicate the 95-th percentile amplitude from an ensemble of 10000 AR(1) model simulations. (c) Normalised histograms of SubNiño4 and Niño 3.4 with mean (μ), standard deviation (σ), skewness (g_1) and excess kurtosis (β_2).

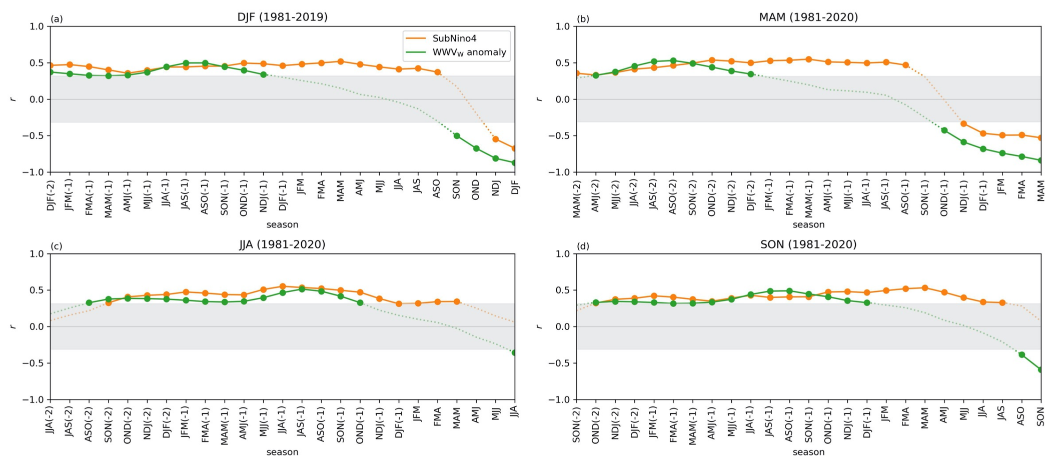

Figure 2 (a) Correlations (r) between Niño 3.4 in DJF and SubNiño4 (orange) and WWV_W anomaly (green) in the 25 overlapping 3-month periods immediately prior. (b) Same as (a) but for MAM. (c) Same as (a) but for JJA. (d) Same as (a) but for SON. (a—d) Correlations with $p < 0.05$ are indicated with solid dot markers connected with solid line. Grey shading indicates correlation levels with $p \geq 0.05$.

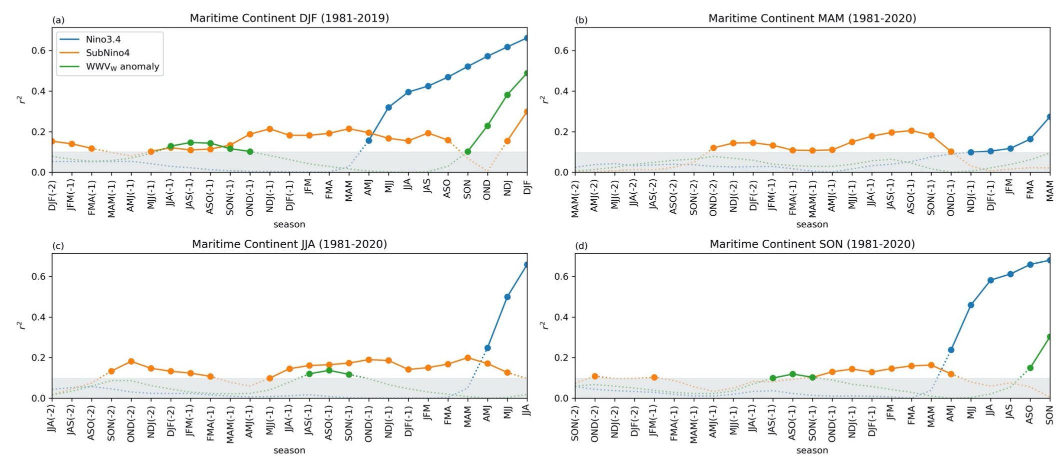

Figure 3 Correlations (r^2) between Maritime Continent precipitation in DJF and SubNiño4 (orange), WWVW anomaly (green) and Niño 3.4 (blue) in the 25 overlapping 3-month periods immediately prior. (b) Same as (a) but for MAM. (c) Same as (a) but for JJA. (d) Same as (a) but for SON. (a—d) Correlations with $p < 0.05$ are indicated with solid dot markers connected with solid line. Grey shading indicates correlation levels with $p \geq 0.05$.

of each main season, the SubNiño4 index is significantly correlated with the Niño 3.4 index over the main season. This long-range correlation is robust across the four main seasons and various lead times, with the correlation coefficient generally staying above 0.4. The SubNiño4 index correlations are more stable with lead time than the widely used WWV_W, decreasing much less at shorter lead times.

The SubNiño4 index captures the subsurface heat advection around half-way between the mature El Niño and La Niña phases of the ENSO cycle. A further merit of the SubNiño4 index over WWV_W is that unlike the latter, the (Sub)Niño4 region is completely free of land, making it more directly relevant to the ocean dynamics. The SubNiño4 index is then a practical and stable index that captures well-known ENSO physics and can serve as a long-range indicator of surface ENSO and thus atmospheric phenomena driven by it.

Atmospheric teleconnections

Over the Maritime Continent, the precipitation and ENSO signal are anti-correlated throughout the year. Fig. 3 shows the correlation coefficients (r^2) between the precipitation over the Maritime Continent in the four main seasons and the Niño 3.4 and SubNiño4 indices and the WWV_W anomaly. SubNiño4 becomes significantly correlated with precipitation much earlier than Niño 3.4. The WWV_W anomaly in general gives weaker correlations than SubNiño4 with precipitation in all four main seasons. It fails to correlate significantly with precipitation in MAM while in the other three main seasons significance is sustained over a much smaller window of lead times compared to SubNiño4.

Similar patterns are also found for precipitations throughout the tropics in the seasons when ENSO is known to play a major role in their interannual modulations, including the wet seasons in Northeast Brazil, West Africa and South Africa and the short rains season of East Africa. ENSO exerts little influence on the precipitation over the long rains season of East Africa and correspondingly insignificant correlations were observed between SubNiño4 and precipitation. This confirms that the SubT atmospheric teleconnection is via the subsurface ENSO cycle and then the surface ENSO state.

In addition to tropical precipitations, SubNiño4 also gives similar correlation patterns with fires over the peak seasons of both Continental and Maritime Southeast Asia, which have distinct annual fire cycles. Again, the lagged correlations afforded by SubNiño4 are more stable than WWV_W. Furthermore, Sparks et al. [10] constructed an index similar to the SubNiño4 and showed that it is capable of predicting tropical cyclone landfall in South China with a lead time of one year. These show the potential value and viability of the SubNiño4 index as a long-range indicator of a variety of atmospheric phenomena driven by ENSO.

References

[1] Wang, C. (2018), *Natl. Sci. Rev.* **5**(6).
[2] Timmermann, A. *et al.* (2018), *Nature* **559**(7715).
[3] Davey, Y. *et al.* (2014), *Clim. Risk Manag.* **1**.
[4] Drosdowsky, W. (2006), *Geophys. Res. Lett.* **33**(3).
[5] Petrova, D. *et al.* (2017), *Clim. Dyn.* **48**(3–4).
[6] Petrova, D. *et al.* (2020), *J. Clim.* **33**(1).
[7] Zhao, S. (2021), *Geophys. Res. Lett.* **48**(19).
[8] Izumo, T. *et al.* (2019), *Clim. Dyn.* **52**(5–6).
[9] Planton, Y. *et al.* (2018), *Geophys. Res. Lett.* **45**(18).
[10] Sparks, N. *et al.* (2020), *Commun. Earth Environ.* **1**(1).

Publication

https://doi.org/10.1002/qj.4290

LEVERHULME
Centre for **Wildfires**, **Environment** and **Society**